Insight into organic reactions from the direct random phase approximation and its corrections

Adrienn Ruzsinszky, Igor Ying Zhang, and Matthias Scheffler

Citation: The Journal of Chemical Physics **143**, 144115 (2015); doi: 10.1063/1.4932306
View online: http://dx.doi.org/10.1063/1.4932306
View Table of Contents: http://scitation.aip.org/content/aip/journal/jcp/143/14?ver=pdfcov
Published by the AIP Publishing

Insight into organic reactions from the direct random phase approximation and its corrections

Adrienn Ruzsinszky,[1] Igor Ying Zhang,[2] and Matthias Scheffler[2]
[1]*Department of Physics, Temple University, Philadelphia, Pennsylvania 19122, USA*
[2]*Fritz-Haber-Institut der Max-Planck-Gesellschaft, Faradayweg 4-6, 14195 Berlin, Germany*

(Received 28 May 2015; accepted 22 September 2015; published online 14 October 2015)

The performance of the random phase approximation (RPA) and beyond-RPA approximations for the treatment of electron correlation is benchmarked on three different molecular test sets. The test sets are chosen to represent three typical sources of error which can contribute to the failure of most density functional approximations in chemical reactions. The first test set (atomization and *n*-homodesmotic reactions) offers a gradually increasing balance of error from the chemical environment. The second test set (Diels-Alder reaction cycloaddition = DARC) reflects more the effect of weak dispersion interactions in chemical reactions. Finally, the third test set (self-interaction error 11 = SIE11) represents reactions which are exposed to noticeable self-interaction errors. This work seeks to answer whether any one of the many-body approximations considered here successfully addresses all these challenges. © *2015 AIP Publishing LLC.* [http://dx.doi.org/10.1063/1.4932306]

INTRODUCTION

In the recent decade, density functional theory (DFT) has experienced a tremendous success in materials physics and chemistry.[1,2] Among the density functional approximations (DFAs), the B3LYP hybrid density functional is especially frequently used in organic chemistry. In spite of the popularity of B3LYP,[3] its reliability has been questioned for organic reactions and isomerization energies.[4–10] There is growing evidence, showing that conventional (semi-)local or hybrid DFAs cannot provide a satisfactory description of several heavily used reaction processes in organic chemistry, for example, hydrocarbon reactions and isomerization reactions.[10–13]

The error in DFAs generally can be traced back to the lack of long-range dispersion effects and unphysical self-interaction.[14–18] In this work, we have chosen representative tests sets which are challenging for one of these reasons for most electronic structure approximations.

Dispersion or van der Waals interactions arise from instantaneous electronic charge fluctuations between different species.[19] This is a long-range attraction and ubiquitous in materials science. The van der Waals interaction is much weaker in strength than a normal chemical bond, but it has important effects on the properties of materials. Semilocal DFA is lacking this long-range correlation interaction. Many theoretical methods, including configuration interaction, many-body perturbation theory, and coupled-cluster (CC) methods, have been developed to estimate this effect. These methods are highly accurate but computationally expensive.

Illustrative examples for the lack of dispersion in organic chemistry include large underestimation of energies associated with alkane bond separation reactions and poor general description of intramolecular dispersion in hydrocarbons. For isomerization reactions, Grimme showed that the error is significantly lowered when DFT-D is used.[16–18] Intramolecular (mainly medium-range) dispersion interactions account in some cases for more than 50% of the isomerization energy.

The random phase approximation (RPA) accounts for dispersion effects in a seamless way but suffers from self-interaction in its correlation component.[19] Self-interaction error and delocalization error are often synonyms in the literature.[20] The source of self-interaction error is the localized nature of the approximate semilocal exchange-correlation (xc) hole. In addition to dispersion effects, the self-interaction error is another lasting problem in most DFAs.[14,20–22] This is an unphysical interaction of the electrons with themselves. Such error originates from the Hartree approximation and should, in principle, be completely canceled out by the *xc* functional. A paradigmatic example of the self-interaction error is the dissociation limit of the one-electron system H_2^+. In this case, by definition, the state with the charge symmetry $H^{+0.5} \cdots H^{+0.5}$ is degenerate with any other symmetry broken states $H^{+q} \cdots H^{1-q}$ with $0 \leq q \leq 1$ and $q \neq +0.5$.[14,21] However, all semilocal DFAs strongly prefer the symmetric solution. Therefore, the self-interaction error in semilocal DFAs is also named as *delocalization* error,[20–22] which has been linked to the wrong convex behavior of the total energy of fractional-charge systems calculated with semilocal DFAs. This concept generalizes the concept of the self-interaction error to many-electron systems.[14,20] A related issue in DFA is the so-called *localization* error, arising from an improper description of fractional spins.[20,21] The *localization* error can be explained by the illustrative example of the dissociation limit of the two-electron system H_2,[20] because the semilocal DFAs prefer the symmetry broken state with an integer-spin distribution on each center to the symmetric closed-shell state with fractional spins on each center. The *localization* error is thus related to the (near)-degeneracy static correlation.[23]

The RPA is composed of the exact exchange and the RPA correlation. The exact exchange completely cancels out the unphysical self-interaction for any one-electron systems as does the Hartree-Fock (HF) method. However, RPA still exhibits a serious *delocalization* (or self-interaction) error in the H_2^+ dissociation limit,[24] because the RPA correlation is nonzero for one-electron systems. This error is also called "self-correlation." In organic radicals and transition states, the delocalization error is known to be noticeable,[21] but it appears in neutral molecules as well.[15]

Although lack of dispersion effects and delocalization error are relevant in organic reactions, the failure of DFA for large molecules cannot simply be traced back to either or both.[10] In the work of Wodrich, *et al.*[25] systematic errors of DFA were found in the evaluation of the stabilizing 1,3-alkyl-alkyl interactions (protobranching) that exist in linear, branched, and most cyclo-alkanes, but not in methane and ethane. The DFA errors were found larger with more-different bonding situations.[10–12,25,26] In related examples, increasing DFA errors of semilocal or global hybrid approximations have been found with increasing hydrocarbon system size for the isomers with the largest number of single bonds and small rings. The errors from different effects accumulate with increasing size.[25,26] This error accumulation manifests especially strongly in atomization energy calculations. The calculated atomization energy errors increase the most with the system size,[5,26,27] because in atomization processes the reactants (molecules) and the products (atoms) show the largest difference possible in the chemical structure. On the other hand, due to the erroneous short-range correlation component, RPA has been known for inaccurate atomization energies.[28,29] Reliable enthalpies of formation for both reactants and products can be obtained from RPA in typical chemical reactions, in which the errors (self-interaction error and dispersions effects) are adequately balanced.

The aim of this work is to provide an assessment of recent many-body, mostly "beyond-RPA," approximations from the aspect of dispersion, self-interaction, and chemical structure difference between reactants and products, respectively, and simultaneously in certain reaction processes.

METHODOLOGY

With a recent efficient implementation, the RPA in a density functional context[30] is becoming a promising ground-state density functional for routine use. Results for structures and molecular properties within RPA are on par with traditional semilocal functionals, and a large improvement has been observed for dispersion-bound systems.[19]

Within density functional theory, the RPA is regarded as being at the highest rung in the hierarchy of density functional approximations.[28] By its nonlocal nature, the RPA includes the exact exchange, and its correlation describes van der Waals interactions as well.

In the DFA context, RPA can be derived from the adiabatic-connection fluctuation dissipation (ACFD) theorem,[30,31] whereby the RPA correlation energy is expressed as

$$E_c = -\frac{1}{2\pi}\int_0^1 d\lambda \int_0^\infty d\omega \times \iint dr dr' v(r,r')\left[\chi_\lambda^{RPA}(r',r;i\omega) - \chi_0(r',r;i\omega)\right]. \quad (1)$$

$\chi_0(r',r;i\omega)$ is the Kohn-Sham (KS) independent-particle density-response function, expressed as

$$\chi_0(r',r,i\omega) = \sum_{ia}\left[\frac{\psi_i^*(r)\psi_a(r)\psi_i(r')\psi_a^*(r')}{\varepsilon_i - \varepsilon_a - i\omega} + c.c\right]. \quad (2)$$

The ACFD theorem is coupled with the Dyson equation

$$\chi_\lambda^{RPA} = [1 - \chi_0(v_\lambda + f_{xc}^\lambda)]^{-1}\chi_0. \quad (3)$$

$v_\lambda = \lambda v = \lambda/|\vec{r}' - \vec{r}|$ is the Coulomb-kernel. $\chi_\lambda^{RPA}(r',r;i\omega)$ is the interacting response function the system with scaled interaction and fixed density. In time-dependent DFT (TDDFT), the neutral excitation energies of the system are found as poles of Equation (2) along the real-frequency axis. The direct RPA (or simply "RPA") sets the exchange-correlation kernel $f_{xc}^\lambda(\vec{r},\vec{r}',\omega)$ to zero.

An accurate computation of energy differences in DFA often profits from a noticeable error cancellation.[32–34] Semilocal functionals have this property, but higher-level density functionals like nonempirical hyper-GGA's and RPA do not.[32] RPA describes the long-range correlation accurately, but its short-range correlation is not adequate. Energy differences with a change in the number of electron pairs pose a problem for RPA.[29,35] In situations where the use of the exact exchange is necessary, the semilocal correlation and exact exchange give a poor performance for energy differences. The RPA+ approximation takes the difference of the beyond-RPA and RPA construction of a semilocal functional, usually GGA or LDA,[35]

$$E_c^{RPA+} = E_c^{RPA} + E_c^{sl} - E_c^{sl\_RPA}, \quad (4)$$

where E_c^{sl} means the correlation energy by a semilocal density functional and $E_c^{sl\_RPA}$ the correlation energy from the RPA parametrization of the same semilocal density functional approximation.

This approach works well for the energy of free atoms or ions but does not have the capability to give accuracy for the molecule where the exact exchange is more diffuse and requires also a more nonlocal correlation. This deficiency appears very strongly in atomization energy calculations, where RPA+ becomes even worse than RPA. The accuracy of the RPA can be improved by taking other different approaches beyond-RPA.[36] The beyond-RPA approximations that rely on many-body theory depend upon the relation of the RPA method to coupled-cluster theory.[37]

In 2008, Scuseria and coworkers pointed out the relation of the RPA and the ring-CC method.[38] The RPA correlation energy in this ring-CCD formulation is then given by

$$E_c^{RPA} = \frac{1}{2}Tr(BT) = \frac{1}{2}\sum_{ij,ab}\langle ij\,|\,ab\rangle T_{jb,ia}, \quad (5)$$

where $\boldsymbol{B}$ is the non-antisymmetrized two-electron repulsion integral matrix defined by the $B_{ia,jb} = \langle ij\,|\,ab\rangle$ four-index matrix elements, and $\boldsymbol{T}$ is the double excitation amplitude matrix in the Riccati equation for CCD. This form is often

called direct RPA in the quantum chemistry literature to emphasize the fact that higher-order exchange-type contributions are not included. From the perturbation theory's aspect, the RPA corresponds to a summed-up series to infinite order. The leading term in the RPA series expansion corresponds to the second-order direct term in Møller-Plesset perturbation theory (MP2).

The SOSEX (second-order screened exchange)[39,40] correction is a possible route to go beyond RPA. The SOSEX correlation energy can be conveniently introduced by antisymmetrizing the Coulomb integral in Eq. (5),

$$E_c^{SOSEX} = \frac{1}{2}Tr((\tilde{B} - B)T) = -\frac{1}{2}\sum_{ij,ab} \langle\, ij \mid ba \,\rangle T_{jb,ia}, \quad (6)$$

where

$$\tilde{B}_{ia,jb} = \langle ij \,\|\, ab\rangle = \langle\, ij \mid ab \,\rangle - \langle\, ij \mid ba \,\rangle\,. \quad (7)$$

The SOSEX-corrected RPA correlation energy takes the following form

$$E_c^{RPA+SOSEX} = \frac{1}{2}Tr(\tilde{B}T) = \frac{1}{2}\sum_{ij,ab} \langle\, ij \,\|\, ab \,\rangle T_{jb,ia}. \quad (8)$$

While the leading term in the RPA series corresponds to the second-order direct term in Rayleigh-Schrödinger perturbation theory, the leading term in SOSEX corresponds to the second-order exchange energy.

The SOSEX itself can be expanded in an infinite series. The leading term in the Rayleigh-Schrödinger perturbation series is the second-order exchange.

The SOSEX is one of the most successful beyond-RPA methods so far. It does not diverge for small-gap, but SOSEX reaction-barrier heights are less accurate than the RPA ones.

The accuracy of RPA can be further boosted by complementing the RPA correlation energy with a correction term arising from single excitations (SEs),[41]

$$\sum_{ia} \frac{\left|\left\langle \psi_i \middle| \hat{f} \middle| \psi_a \right\rangle\right|^2}{\varepsilon_i - \varepsilon_a}. \quad (9)$$

In this expression, $\hat{f}$ is the single-particle Hamiltonian. If the reference potential-field is HF, then $\hat{f}$ is the Fock-operator. i and a denote the occupied and unoccupied orbital space with its wavefunctions and energies. The SE term is zero for a HF reference and therefore is not included in MP2. Generally, in second-order perturbation theory, all terms the (the RPA correlation energy, SE, and SOSEX) contribute.

Without a renormalization, this theory suffers from the divergence problem as does 2nd-order Møller-Plesset perturbation theory for metallic systems when the single particle KS gap closes. Including all terms to infinite order, this series can be renormalized SE (rSE), as RPA itself is already renormalized.[41]

The renormalized second-order perturbation theory (rPT2) is the most balanced approach beyond RPA.[41] rPT2 includes three components: direct Coulomb, the second-order, and the single excitations. In rPT2, all these terms are summed-up to infinite order. By the infinite summation, the rPT2 fixes the anomalies of bare second-order perturbation theory by renormalizing the leading terms for the direct Coulomb, the second-order, and the single excitations. rPT2 is exact to second-order for the energy.

There are a significant number of attempts recently to improve RPA atomization energies and other chemical properties as well. Most of these approximations account for the exchange interaction in RPA correlation and go beyond the SOSEX approximation. One of them is the rPT2 described above, but other approaches like RPAX2[42,43] and the recently developed RPAx-SO2[44] deliver also improvement beyond RPA. The AXK (approximate exchange kernel) approach is based on renormalization of the many-body perturbation theory (in a similar manner as rPT2) and provides a leading correction to RPA.[45] Data bases for atomization energies (G2-1, HEAT, AE6)[46–48] and barrier heights (BH76, BH6, HTBH38, and NHTBH38)[47,49–51] used in either case are not exactly compatible. Because of the large variety of data sets, any comparison of these methods should warrant caution. The common feature of all these approaches is their more balanced performance for atomization energies, barrier heights, and weak interactions than SOSEX.

A self-consistent implementation of the RPA within the ACFD framework requires the cumbersome (optimized-effective potential) OEP approach.[52–54] Self-consistent RPA correlation energies have been recently reported by the efficient algorithm of Heßelmann which is based on the CC-like form of the dRPA equations (Riccati equations).[42,43] In our work we use the RPA with the ACFD framework in a non self-consistent manner. The non-self-consistent energies are called RPA@DFA or (EXX + cRPA)@DFA in the literature, where EXX + cRPA is an orbital-dependent functional of exact exchange and RPA correlation. In materials applications usually the PBE is chosen as a reference. The same statement applies to other DFAs and they can be applied as references with the same accuracy.

TEST SETS

In this work, we assess the performance of several many-body approximations on hydrocarbon reaction classes. The aim of establishing this classification of reactions is to enable high-accuracy enthalpy of formation calculation for hydrocarbons. Atomization reactions require the highest level of theory. At this time coupled-cluster theory with at least perturbative correction to quadruple excitations (CCSDT(Q)) with complete basis set (CBS) extrapolation, relativistic corrections, and anharmonic zero-point vibrations could deliver the so called subchemical accuracy (0.1 kcal/mol) in comparison with experimental atomization energies. Due to error accumulation with increasing system size, subchemical accuracy at CCSDT(Q) level of theory is not a realistic aim for larger molecules including all these corrections. The RCn test set ("n" stands for the hierarchy of the particular reaction class RC) is designed to assess and compare the accuracy and precision of several selected theoretical electron structure methods. Accurate methods should perform well even for $n = 1$ and should show consistently increasing accuracy with the increase of n. In our reaction energy calculations, only

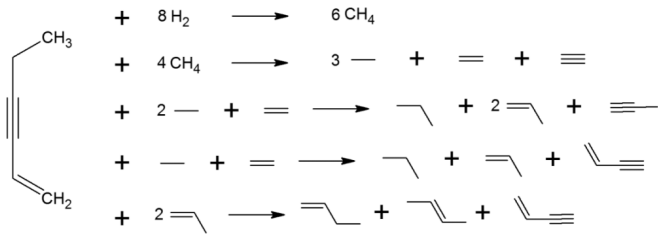

FIG. 1. RC1-5 reactions.

the CBS effect is considered. Then our reaction energies are directly comparable to the reference CCSD(T) CBS extrapolated energies, which also neglect relativistic and zero-point-vibration effects.[55]

The hydrocarbon test sets from reaction classes RC1-RC5 provide a convenient hierarchy of reaction classes.[56] Each of these successively conserves larger molecular fragments in the products. A special so-called RC0 class contains the atomization reactions of selected hydrocarbons, as the atoms are smallest possible molecular fragments. Sketches of these reactions are shown in Figure 1.

Isogyric reaction class (RC1) conserves the total number of electron pairs in bond separation reactions of hydrocarbons with hydrogen molecules, which results in methane as the only product.[57] In the isodesmic class of reactions (RC2), the bond multiplicities (single, double, and triple) are also conserved.[57–59] This class contains the bond separation reactions of hydrocarbons with methane molecules yielding diatomic ethane, ethene, and ethyne molecules. In hypohomodesmotic reactions (RC3), there are equal numbers of carbon atoms in their various states of hybridization on both sides of the reaction equation, and equal numbers of carbon atoms with zero, one, two, and three hydrogens attached in the reactants and products.[60,61] In homodesmotic (RC4) reactions, there are equal numbers of each type of carbon-carbon bond in the reactants and products and equal numbers of each type of carbon atom with zero, one, two, and three hydrogens attached in reactants and products.[62] By design, the reaction energy of the homodesmotic reaction is very small, usually lower than 0.5 kcal/mol. Therefore, the homodesmotic reaction provides a critical criterion to benchmark the electronic structure methods with different levels of approximation. Homodesmotic reactions provide a good error cancellation between some small molecules and a large molecule. Accurate (or near exact) atomization energies are unfeasible for large molecules because of the huge computational demand.

Hyperhomodesmotic reaction class (RC5) contains the reaction with highest similarity between reactants and products.[63] In this class of reactions, there are equal numbers of carbon-carbon bond types on both reactants and products and equal numbers of each type of carbon atom with zero, one, two, and three hydrogens attached in the reactants and products.

The Diels-Alder reaction cycloaddition (DARC) set suggested by Johnson *et al.* provides an even more stringent test for DFAs.[64,65] It contains 14 representative Diels-Alder reactions, namely, the reactions of butadiene, cyclopentadiene, cyclohexadiene, and furane with typical dienophiles such as ethene, ethyne, maleic anhydride, and maleimide (see Fig. 2).

In this set of reactions, delocalization errors and errors from nonbonded intramolecular attractions show up simultaneously in the bicyclic and tricyclic reaction products. Most semilocal density functionals were found to underbind the bicyclic tricyclic reaction products. The source of energy errors of DFAs for the products is related to the tendency of most approximations to underestimate nonbonded intramolecular attractions. Apart from the missing dispersion effects, the delocalization error of semilocal DFAs causes underbinding of the reaction energies, i.e., it puts the energy of the products too high relative to the energy of the reactants. As an evidence for

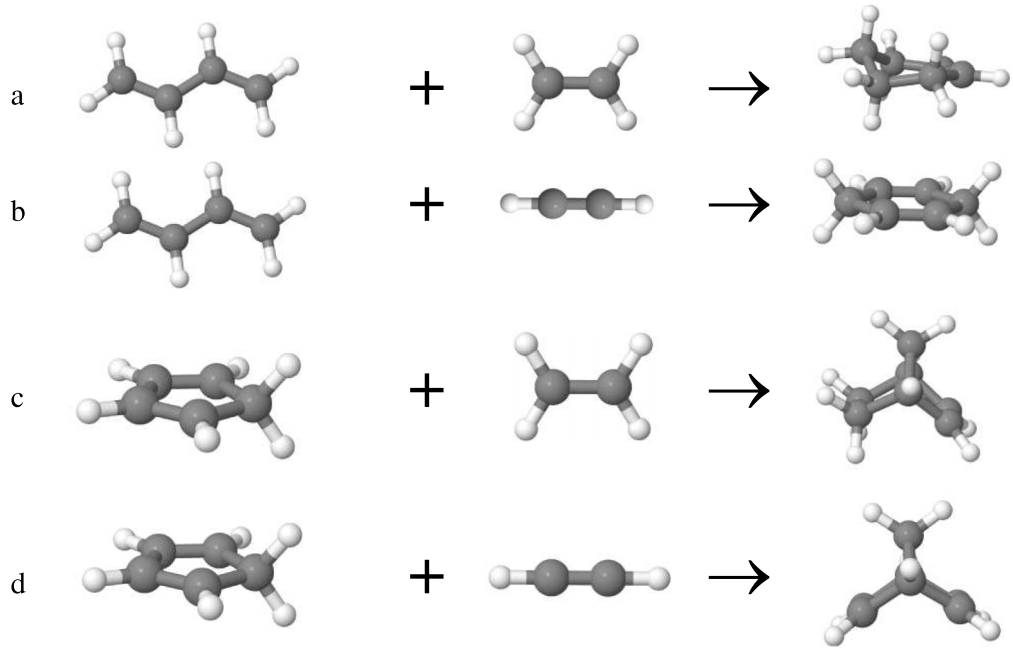

FIG. 2. Illustration of the selected four reactions in the DARC dataset. (a) butadiene + ethene → P1 (R1), (b) butadiene + ethane → P2 (R2), (c) cyclopentadiene + ethane → P3 (R3), (d) cyclopentadiene + ethane → P4 (R4).

the importance of the delocalization error for these reactions, Johnson and coworkers found systematic improvement in the calculated reaction energies with the screened hybrid CAM-B3LYP and local hybrid MCY3, a class of functionals which showed signs of improvement in the description of fractional numbers of electrons.[65] Johnson *et al.* supposed that, in the DARC test set, the delocalization error of semilocal DFAs lowers the energy of the reactants and the lack of intramolecular dispersion interaction effects increases the energy of the products, and these two effects lead to the above mentioned typical underbinding. The underbinding can be corrected by *a posteriori* dispersion correction and by inclusion of a fraction of exact exchange.

The last test set completes the variety of possible error sources in electronic structure calculations. Reaction equations are shown in Table VII. The self-interaction error 11 (SIE11) subset includes 11 systems.[64] Five of these are positively charged, and seven systems are neutral. As reaction types, one of the reactions is an isomerization, while all others are dissociations. Charged molecules or radicals could be challenging for semilocal density functionals, due to the self-interaction error.

BASIS SET

A well-known challenge in many-body approximations is their sensitivity to basis sets and the slow convergence of their correlation energy with increasing basis set quality. This slow convergence is due to the difficulty of using smooth orbital product expansions to describe the electron–electron Coulomb cusps in real space.[66,67] One possible way to address the slow basis-set convergence can be the basis-set extrapolation. The complete or infinite basis set values are extrapolated from smaller basis set values for the property in question. The most widely used scheme is Dunning's polarized valence-correlation consistent Gaussian-type orbital (GTO) basis sets (aug-cc-pVnZ) with $n = 2,3,4,5$, and higher. "n" equals the highest angular number "l_{max}" in the so-called correlation consistent (cc) polarized valence (pV) basis set.

All-electron calculations on RPA correlation energies revealed that core and valence correlation contributions converge differently in RPA.[68,69] The (numerical atom-centered orbital) NAO-valence-correlation consistency (VCC)-nZ basis sets are suitable for converging electronic total-energy calculations based on valence-only (frozen-core) correlation methods which contain explicit sums over unoccupied states (e.g., the RPA or second-order Møller–Plesset perturbation theory).[70] The advantage of NAO-VCC-nZ over GTO basis sets such as the Dunning "cc" basis sets is that, with NAOs, both the behavior near the nucleus and that for the tails of orbitals far away from atoms are much more physical.

In this work, we used the NAO basis sets with VCC, termed NAO-VCC-nZ. Here, the index "nZ" refers to the number of basis functions used for the valence shell with $n = 2$, 3, 4, 5. These basis sets are constructed analogous to Dunning's cc-pVnZ but utilize the more flexible shape of NAOs.[71,72] Similar to Dunning's basis sets, the basis set incompleteness error can be gradually reduced with the increase of the index "n" and can be removed using two point extrapolation schemes. In the NAO basis set, the free atomic radial potential is used to generate the radial functions used in the minimal basis set. In addition to the minimal basis set, the NAO adds three subsets: the polarization set, the correlation set, and the enhanced minimal basis set. The subsets employ radial functions constructed from hydrogen-like orbitals generated by hydrogen-like radial potentials The n principal quantum number of the radial functions generates $n = l + 1$ basis functions using equation $\varphi_i = \frac{u_i(r)}{r} Y_{lm}(\Omega)$. The NAO's construction concept is then the same as Dunning's valence correlation correlation consistency: the polarization set is constructed by adding numeric hydrogen-like orbitals with increasing l number with the increase of the basis set.

COMPUTATIONAL DETAILS

In this part of the work, the technical details of the calculations focus on the choice of basis sets and grid points.

(a) Auxiliary basis set

The common feature of MP2, RPA, and *GW* methods is that they require the explicit inclusion of unoccupied single-particle states. As a consequence, noticeably larger basis sets are needed to obtain converged results in these calculations.[29] Therefore, the computational effort of these methods can be significant.

The evaluation of the four-center integrals in the Coulomb integral is computationally challenging within the NAO formalism. The same computational problem appears also in the evaluation of the screened Coulomb interaction W and χ_0. The RPA implementation in FHI-aims electronic structure code[73,74] is based on the resolution of the identity (RI) technique combined with an appropriate basis set is a powerful choice for the calculation of four-center integrals.[75]

The basic idea of the RI is based on the expression of the product of the Kohn-Sham orbitals,

$$\varphi_i^*(\vec{r})\varphi_j(\vec{r}) = \sum_{\mu=1}^{N_{aux}} C_{ij}^{\mu} P_{\mu}(\vec{r}). \tag{10}$$

In the expression $P_\mu(\vec{r})$ are the auxiliary basis functions, $C_{ij}^{\mu}(\vec{r})$ are the expansion coefficients, and N_{aux} is the size of the auxiliary basis set. In this work, the auxiliary basis was constructed as the "on-site" pair products of the regular basis functions. The auxiliary basis function is an atom-centered function with radial and angular contributions: $P_\mu(\vec{r}) = \frac{\xi(\vec{r})_{nl}}{\vec{r}} Y_{lm}(\vartheta,\varphi)$. The number of these pair products can be controlled in the program. These products of the regular orbitals are then orthonormalized at each atom using the Gram-Schmidt method. The number of the auxiliary pairs then is set by the number of the regular basis set and the accuracy of the orthonormalization. In the current implementation, the C_{ij}^{μ} coefficients are found by minimizing the error of the expansion of Equation (10) with respect to $\vec{r}$ and $\vec{r}'$ (density fitting). The minimization of error follows two different routes in the code. In the current work, we selected the "RI-V" variant of the RI method in which the 4-center integrals were calculated as

$$(ij|kl) = \sum_{\mu\nu} C_{ij}^{\mu}(\mu|\nu) C_{ikl}^{\nu} \tag{11}$$

and

$$(\mu|\nu) = V_{\mu\nu} = \int \frac{P_\mu(\vec{r})P_\nu(\vec{r}')}{|\vec{r}-\vec{r}'|} dr dr', \quad (12)$$

where i, j, k, and l are the notations of the Kohn-Sham basis functions, and μ, ν denote the auxiliary basis functions. By utilizing the auxiliary basis functions, the N_{basis}^4 4-center integrals are reduced to $N_{basis}^2 \cdot N_{aux}$ 3-center integrals and N_{aux}^2 2-center integrals (where N_{basis} and N_{aux} are the numbers of NAO basis functions and auxiliary basis functions, respectively). With appropriate auxiliary basis sets, the computational effort can be significantly reduced and allows an accelerated numerical integration in the RPA correlation energy.

The NAO basis functions are strictly localized in a finite spatial area around the nuclei, and the extent of this area is controlled by a confining potential. From an earlier work of Ren *et al.*,[74] one can see that increasing the onset radius of the confining potential (i.e., enlarging the extent of the NAO basis functions) from the default value (4 Å) has little effect on the convergence behavior.

b. Basis set extrapolation

For all calculations, we use NAO-VCC-nZ with cardinal numbers: $n = \{3,4\}$, constructed according to Dunning's "correlation consistent" recipe.

A popular CBS extrapolation scheme[29,75,76] is a two-point inverse cubic extrapolation of total energies, suggested for RPA and MP2.[76] Our preliminary results show that such a formula might be useful for $n = \{6,7\}$. The size of most molecules tested here does not allow the use of these larger basis sets. On the other hand, extrapolation from $n = \{3,4\}$ only does not give sufficient accuracy. This statement is seemingly in opposition to some observations for the basis set convergence for RPA energy differences. Reference 77 suggests for relative energies of alkane conformers, the IDISP, the ISO34, and the G2RC sets,[64] and RPA energy differences are essentially converged at the $n = 4$ basis set level. In these reaction energy test sets, the $n = 4$ basis set errors are comparable to or smaller than RPA method errors for energy differences, and they tend to cancel. However, this error compensation might fail for many other reactions as the RPA energies are very far from being converged at $n = 4$ level.

We suggest to extrapolate the exact exchange noted as EXX and various correlation energies (RPAc or PT2c as a general notation for the "beyond-RPA" correlation energies) separately as

$$E_{CBS}^{EXX} = E_{4Z}^{EXX} + \alpha\left(E_{4Z}^{EXX} - E_{3Z}^{EXX}\right) \quad (13)$$

and

$$E_{CBS}^{PT2c} = E_{4Z}^{PT2c} + \beta\left(E_{4Z}^{PT2c} - E_{3Z}^{PT2c}\right), \quad (14)$$

where E_{CBS}^{EXX} is the estimated exact EX@CBS, E_{4Z}^{EXX} is the EXX@NAO-VCC-4Z energy, etc. The extrapolation parameters found to be $\alpha = 0.191$ for exact EXX, and $\beta = 1.141, 1.137, 1.086$, and 1.125 for RPA, RPA+, RPA + SOSEX, and rPT2 correlation, respectively, as explained below.

Now we will explain how to estimate α and β in Equations (13) and (14). In order to study basis set dependence, Ref. 78 calculated the RPA energies of 65 hydrocarbons from CH_4 to C_6H_6 with increasing cardinal numbers: $n = \{3,4,5,6\}$ with Dunning aug-cc-pVnZ (AnZ) basis sets. The m exponent was fitted in the following formula to describe the convergence of the RPA correlation energies,

$$E_{AnZ}^{RPAc} = E_{CBS}^{RPAc} + An^{-m}. \quad (15)$$

Notice that an $1/n^3$ formula was originally proposed for the correlation and total energies.[78–80] However, the inverse cubic formula might lead to large extrapolated energy errors for $n = 3$ and 4.[81] Optimization of the inverse power exponent, m, leads to considerable improvements for the RPA correlation energy term.[82] For obtaining the optimal value of m, we use E_{3Z}^{RPAc}, E_{4Z}^{RPAc}, and E_{5Z}^{RPAc} (the calculation of the E_{6Z}^{RPA} is beyond the possibilities due to the computational requirements). Even calculations of E_{5Z}^{RPA} energies were limited to smaller molecules with the beyond-RPA methods. For the complete basis set extrapolation of the RPA correlation energy, Equation (14), we use $\beta[3,4] = \frac{1}{\left(\frac{4}{3}\right)^m - 1}$ for $n = 3$ and 4, where optimal $m = 2.19$. For 2-point extrapolation of the exact exchange, Equation (13), we use $\alpha[3,4] = \frac{1}{\left(\frac{4}{3}\right)^m - 1}$ for $n = 3$ and 4, where $m = 6.36$, is an effective decay exponent obtained by minimizing the root-mean-square deviation (rmsd) from the numerical HF E_{CBS}^{EXX} for the test set proposed by Jensen.[83]

Finally, the extrapolated total energy is estimated as the sum of the results of Equations (13) and (14). The total energies compared to the reference energies and the deviations ($E_{\text{calc.}} - E_{\text{ref.}}$) are shown in the following tables.

c. The grid

The FHI-aims code integrates its Hamiltonian matrix elements numerically on a grid. FHI-aims is an all-electron code, which treats all electronic states (core and valence) on the same footing.[73] In FHI-aims, each atom gets a series of radial spheres (*shells*) around it and distributes a certain number of actual grid points on each shell. The number of radial shells is controlled by "radial base" referring to the number of radial shells and the confinement potential in the radial Schrödinger equation. The "radial multiplier" controls the density of the radial shells by adding additional shells between the ones fixed in "radial base." Our setting corresponds to "tight" or 1 μH convergence.

The distribution of actual grid points on the radial shells is done using so-called Lebedev grids, which are designed to integrate all angular momenta up to a certain order l exactly. Angular grid points come with fixed numbers of grid points. Fewer grid points are necessary on the inner radial shells, but a suitably increased outer grid value is needed for better accuracy. A "tight" setting corresponds to at least "434" in the outer shells. In our work for the small energy differences, we use a tight setting of the outer grid points.

RESULTS AND DISCUSSION

The very bottom of the homodesmotic hierarchy is the atomization reactions (RC0). The accuracy of a given method should reflect in small errors, and more importantly, the errors should decrease with the hierarchy rank number n, the indicator of the increased hierarchy. In the RC0 class, no electron pairs are conserved at all in reactants and products. In

TABLE I. The deviations of CBS extrapolated atomization energies from reference energies[56] for 12 hydrocarbon molecules. RC0A, B, and C are used for atomization energy of a group of reactions. Errors are given in kcal/mol. The acronyms for Tables I–VII are the following: MD: Mean deviation, MAD: Mean absolute deviation, CSSD: Corrected sample standard deviation, Min: Minimum, Max: Maximum.

	Reactions	Reference	RPA	RPA+	RPA+SOSEX	RPA+rSE	rPT2
RC0A	1	1310.67	−56.87	−62.50	−4.72	−45.44	7.11
	2	996.80	−54.43	−59.43	−9.08	−42.54	3.15
	3	1153.25	−55.79	−61.10	−7.07	−44.36	4.73
	4	1151.42	−55.24	−60.52	−7.11	−43.98	4.53
	5	1605.44	−68.26	−75.25	−4.48	−54.79	9.48
RC0B	1	1598.6	−58.96	−65.21	1.35	−49.39	11.38
	2	1451.56	−57.78	−63.69	−1.89	−47.54	8.76
	3	1294.89	−56.22	−61.79	−4.07	−46.20	6.36
	4	1453.66	−57.94	−63.88	−1.67	−47.61	9.10
	5	1298.89	−56.43	−62.07	−3.22	−46.20	7.43
RC0C	1	1181.88	−55.56	−61.55	−3.93	−45.14	6.88
	2	1478.57	−68.28	−75.71	−5.34	−55.04	8.35
MD			−58.48	−64.39	−4.27	−47.35	7.27
MAD			58.48	64.39	4.49	47.35	7.27
CSSD			4.74	5.41	2.79	3.97	2.34
Min			−68.28	−75.71	−9.08	−55.04	3.15
Max			−54.43	−59.43	1.35	−42.54	11.38

isogyric reactions (RC1), the number of C bonds is conserved. Because bond breaking is present in this class of reactions, the RC1 class requires a high level of electron correlation theory. Eshuis and Furche reported dRPA/cc-pVTZ (direct RPA) results (input orbitals were obtained using the TPSS functional[84]) for test sets of the RC*n* reaction classes.[59] The RPA atomization energies show large errors and the results are improving toward higher *n*-order reaction classes. The poor RPA atomization energies reflect the unbalanced description of the exchange and correlation holes within RPA.

We consider three sets of hydrocarbons proposed by Wheeler *et al.*[56] The first set consists of conjugated hydrocarbons, the second consists of nonconjugated hydrocarbons, and the third includes two ring structures. In this work, we select 5 hydrocarbons from each set and evaluate the performance of all methods including RPA and beyond-RPA approximations on these molecules for each reaction class. All energies were evaluated at B3LYP/6-31G(d) optimized geometries. In Tables I–VII, we show the renormalized rSEs to demonstrate the effect of all corrections beyond RPA. The RPA@PBE atomization energies (RC0, Table I) for all three sets are just as poor as shown in the work of Eshuis and Furche. The RPA+ approach does not improve beyond RPA for atomization energies. These results are consistent with

TABLE II. The deviations of CBS extrapolated isogyric (RC1) reaction energies from reference energies[56] for 12 hydrocarbon reactions. Errors are given in kcal/mol.

	Reactions	Reference	RPA	RPA+	RPA+SOSEX	RPA+rSE	rPT2
RC1A	1	−133.34	2.76	4.34	−9.28	6.66	−5.37
	2	−226.90	3.15	6.42	−14.12	7.20	−10.09
	3	−180.61	2.82	5.25	−11.86	6.57	−8.13
	4	−182.44	3.37	5.83	−11.90	6.94	−8.33
	5	−149.40	3.49	5.06	−9.90	7.96	−5.42
RC1B	1	−65.72	2.71	2.63	−2.73	5.07	−0.34
	2	−102.61	2.88	3.66	−6.21	5.74	−3.33
	3	−149.13	3.42	5.07	−8.61	5.91	−6.12
	4	−100.51	2.71	3.47	−5.98	5.67	−2.99
	5	−145.12	3.20	4.78	−7.77	5.90	−5.06
RC1C	1	−151.98	3.05	4.80	−8.72	5.78	−5.98
	2	−166.13	2.47	4.11	−10.98	6.55	−6.92
MD			3.00	4.62	−9.01	6.33	−5.67
MAD			3.00	4.62	9.01	6.33	5.67
CSSD			0.33	1.05	3.10	0.80	2.63
Min			2.47	2.63	−14.12	5.07	−10.09
Max			3.49	6.42	−2.73	7.96	−0.34

TABLE III. The deviations of CBS extrapolated isodesmic (RC2) reaction energies from reference energies[56] for 12 hydrocarbon reactions. Errors are given in kcal/mol.

	Reactions	Reference	RPA	RPA+	RPA+SOSEX	RPA+rSE	rPT2
	1	17.45	−1.31	−1.42	1.10	−0.38	2.06
	2	21.89	−3.68	−3.90	1.17	−1.59	3.25
RC2A	3	19.18	−2.63	−2.79	0.97	−1.35	2.26
	4	17.36	−2.09	−2.22	0.92	−0.99	2.04
	5	19.42	−1.13	−1.23	1.35	−0.18	2.33
	1	6.96	−0.04	−0.05	0.22	0.09	0.39
	2	9.42	−0.83	−0.85	0.16	−0.57	0.45
RC2B	3	12.22	−1.98	−2.04	−0.11	−1.59	0.30
	4	11.62	−1.10	−1.14	0.29	−0.74	0.69
	5	16.64	−2.62	−2.74	0.32	−2.01	0.95
RC2C	1	16.84	−1.57	−1.49	2.53	−2.37	1.77
	2	20.73	−2.71	−2.72	1.14	−2.72	1.14
MD			−1.81	−1.88	0.84	−1.20	1.47
MAD			1.81	1.88	0.86	1.21	1.47
CSSD			1.00	1.05	0.72	0.89	0.95
Min			−3.68	−3.90	−0.11	−2.72	0.30
Max			−0.04	−0.05	2.53	0.09	3.25

our knowledge about the exchange-correlation holes in atoms and molecules. The exchange-correlation hole in molecules is more extended. The extended nature of the hole in molecules requires a more long-ranged correlation which is missing in RPA+.

The inclusion of the rSEs has some impact on the quality of atomization energies; however, the deviation from the reference values remains significant. SOSEX corrected RPA improves atomization energies. The rPT2 approximation which corresponds to (RPA+rSE+SOSEX)@PBE deteriorates the quality of results compared to (RPA+ SOSEX) @PBE.

The isogyric class (RC1, Table II) includes bond breaking and making. A significant improvement with RPA can be noticed for this reaction class. The same improvement applies here for RPA+ as well. The more expensive RPA+SOSEX does not reach the accuracy of RPA for this reaction class. Single excitations do not bring improvement. For isogyric reactions, the rPT2 brings poorer performance than RPA and RPA+, reflecting the negative effect of the inclusion of rSE and SOSEX corrections.

A significantly more consistent performance is noticed for the isodesmic (RC2, Table III) class of reactions. In isodesmic reactions, the electron numbers and the bond orders (single, double, and triple) are also conserved. RPA and RPA+ both give results close to chemical accuracy (1 kcal/mol). SOSEX improves beyond RPA, but the rSE has some negative effect which reflects in the accuracy of rPT2. In

TABLE IV. The deviations of CBS extrapolated hypohomodesmotic (RC3) reaction energies from reference energies[56] for 7 hydrocarbon reactions. Errors are given in kcal/mol.

	Reactions	Reference	RPA	RPA+	RPA+SOSEX	RPA+rSE	rPT2
	1	3.30	1.54	1.49	1.19	1.86	1.54
	2	0.14	−0.44	−0.46	−0.43	0.70	0.69
RC3A	3	−0.04	0.48	0.47	−0.06	0.93	0.39
	4	0.67	0.89	0.87	0.45	1.28	0.85
	5	3.18	1.55	1.51	1.19	1.83	1.50
	1	0.13	−0.01	−0.02	0.02	−0.02	0.01
	2	−0.05	0.34	0.33	0.26	0.31	0.23
RC3-4B	3	−0.10	−0.36	−0.37	−0.26	−0.38	−0.28
	4	−0.58	1.31	1.30	0.78	1.21	0.71
	5	−1.25	0.66	0.67	0.30	0.59	0.24
RC3C	1	−4.12	2.06	2.21	2.41	0.40	0.78
	2	−2.32	0.74	0.81	0.76	−0.17	−0.16
MD			0.73	0.73	0.55	0.71	0.54
MAD			0.87	0.88	0.68	0.81	0.62
CSSD			0.78	0.81	0.79	0.74	0.59
Min			−0.44	−0.46	−0.43	−0.38	−0.28
Max			2.06	2.21	2.41	1.86	1.54

TABLE V. The deviations of CBS extrapolated homodesmotic (RC4) reaction energies from reference energies[56] for 12 hydrocarbon reactions. Errors are given in kcal/mol.

	Reactions	Reference	RPA	RPA+	RPA+SOSEX	RPA+rSE	rPT2
	1	0.35	1.07	1.06	0.70	1.04	0.69
	2	1.14	0.61	0.62	0.47	0.57	0.45
RC4A	3	−0.09	0.92	0.91	0.52	0.91	0.54
	4	0.83	1.12	1.10	0.83	1.05	0.79
	5	0.25	1.06	1.05	0.68	0.99	0.63
	1	0.13	−0.01	−0.02	0.02	−0.02	0.01
	2	−0.05	0.34	0.33	0.26	0.31	0.23
RC3-4B	3	−0.10	−0.36	−0.37	−0.26	−0.38	−0.28
	4	−0.58	1.31	1.30	0.78	1.21	0.71
	5	−1.25	0.66	0.67	0.30	0.59	0.24
RC4C	1	−7.40	1.93	2.11	2.24	−0.09	0.26
	2	−5.61	0.62	0.71	0.61	−0.65	−0.67
MD			0.77	0.79	0.60	0.46	0.30
MAD			0.83	0.85	0.64	0.65	0.46
CSSD			0.61	0.64	0.61	0.62	0.44
Min			−0.36	−0.37	−0.26	−0.65	−0.67
Max			1.93	2.11	2.24	1.21	0.79

hypohomodesmotic (RC3, Table IV) reactions, the reactants and products contain equal numbers of carbon atoms in the same formal hybrid states and equal numbers of hydrogen atoms attached. In homodesmotic (RC4, Table V) reactions, the reactants and products contain equal numbers of each type of possible carbon-carbon bonds [C_{sp3}—C_{sp3}, C_{sp3}—C_{sp2}, C_{sp3}—C_{sp}, C_{sp2}—C_{sp2}, C_{sp2}—C_{sp}, C_{sp}—C_{sp}, C_{sp2} = C_{sp2}, C_{sp2}=C_{sp}, C_{sp}=C_{sp}, C_{sp}≡C_{sp}]. In addition in hyperhomodesmotic (RC5, Table VI) reactions, the reactants and products contain equal numbers each type of possible hydrogen-carbon-carbon-hydrogen bonds [H_3C—CH_2, H_3C—CH, H_2C—CH_2, H_3C—C, H_2C—CH, . . .].

For hypohomodesmotic RC3, homodesmotic RC4, and hyperhomodesmotic RC5 chemical reactions, the accuracy of RPA@PBE improves consistently further. Practically, all methods shown here are sufficiently accurate for these reaction classes. The difference between methods becomes increasingly small toward the highest hierarchy RC5 reaction class. Figure 3 confirms that overall the RPA gives the most consistent performance in the increased rank of hierarchy of RC*n* reactions.

A stringent reaction energy test set is the Diels-Alder condensation reactions (DARC test set) that is suitable for analyzing the delocalization and dispersion errors in semilocal DFA such as PBE as discussed earlier. A question we address here is whether the errors of semilocal functionals for the DARC reaction energies arise primarily from the delocalization error of the density or from the underestimation of weak interactions. We conclude that the latter is the source of most of the

TABLE VI. The deviations of CBS extrapolated hyperhomodesmotic (RC5) reaction energies[56] from reference energies for 12 hydrocarbon reactions. Errors are given in kcal/mol.

	Reactions	Reference	RPA	RPA+	RPA+SOSEX	RPA+rSE	rPT2
	1	0.45	0.10	0.10	0.26	0.15	0.31
	2	1.69	0.87	0.88	1.00	0.88	1.03
RC5A	3	0.63	1.01	1.00	0.88	1.06	0.95
	4	0.91	0.16	0.16	0.41	0.18	0.43
	5	0.37	0.59	0.59	0.66	0.62	0.70
	1	−0.03	−0.02	−0.02	0.00	−0.01	0.00
	2	0.09	0.64	0.63	0.47	0.63	0.47
RC5B	3	0.16	−0.46	−0.46	−0.24	−0.45	−0.24
	4	0.10	0.27	0.27	0.20	0.27	0.22
	5	0.11	0.36	0.36	0.40	0.36	0.40
RC5C	1	−6.68	−0.71	−0.49	0.66	−2.55	−1.20
	2	−4.96	−2.03	−1.89	−1.00	−3.13	−2.14
MD			0.07	0.10	0.31	−0.17	0.08
MAD			0.60	0.57	0.51	0.86	0.67
CSSD			0.83	0.78	0.54	1.32	0.91
Min			−2.03	−1.89	−1.00	−3.13	−2.14
Max			1.01	1.00	1.00	1.06	1.03

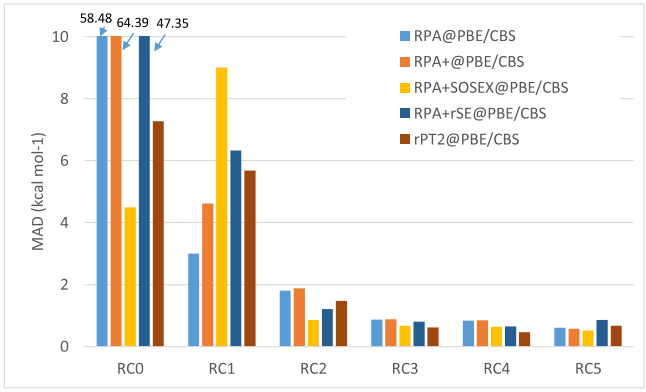

FIG. 3. Mean absolute deviation (MAD) from reference energies[56] of 12 bond separation reaction energies for RPA@PBE, RPA+@PBE, RPA+SOSEX@PBE, RPA+rSE@PBE, and rPT2@PBE theoretical methods. All calculated energies are complete basis set extrapolated (CBS). Abbreviations: RC0, atomization; RC1, isogyric; RC2, isodesmic; RC3, hypoho-modesmotic; RC4, homodesmotic; RC5, hyperhomodesmotic. The RPA and RPA+MAD values for RC0 are over 60 kcal mol^{-1}, as shown in Table I.

error, since RPA calculations with PBE orbitals, which correct the latter error but not the former one, yield much more accurate DARC reaction energies than PBE does. The rSE and SOSEX corrections to RPA (as combined in rPT2) could, if applied self-consistently, remove the delocalization error. However, when applied on PBE or HF orbitals, they actually worsen the DARC reaction energies in comparison to direct RPA.

In order to carry out this analysis, we assess systematically the reaction energies with certain "beyond-RPA" approximations on PBE, PBE0 with 25% EXX mixing, and HF orbitals, respectively. Due to the computational demand of beyond-RPA approximations, we selected four reactions from the DARC test set to assess SOSEX and rPT2 (Figures 2, 4(a), 5, and 6).

It should be noted here that the HF reference is not a straightforward choice for ACFD-RPA and is tested here only to assess the delocalization/localization issue in the DARC test set.[16] If a DFT reference is chosen, the density of the Kohn-Sham system with the exact exchange-correlation potential in principle is the same as the density of the real interacting system. The coupling constant integration makes a smooth connection between the potential of the Kohn-Sham and interacting systems. For the HF reference, the coupling constant integral can be formulated only for a perturbed HF ground-state energy.

In the analysis of the *n*-homodesmotic reaction classes, the RPA and beyond-RPA approximations were used only with PBE Kohn-Sham eigenvalues and orbitals. We found that the PBE reference outperforms other references for the DARC test set. In the case of the reaction energies of the DARC test set, the choice of the input orbitals for the subsequent RPA calculation has a special role in this work. The assessment of reaction energies with respect to different references reveals the density errors of these reactions. In the DARC reactions, two errors of the semilocal functionals (over-delocalization of the electron density and underestimation of weak interaction) could be important. Delocalization error should overstabilize reactants, shifting the reaction energies in the endothermic direction. The

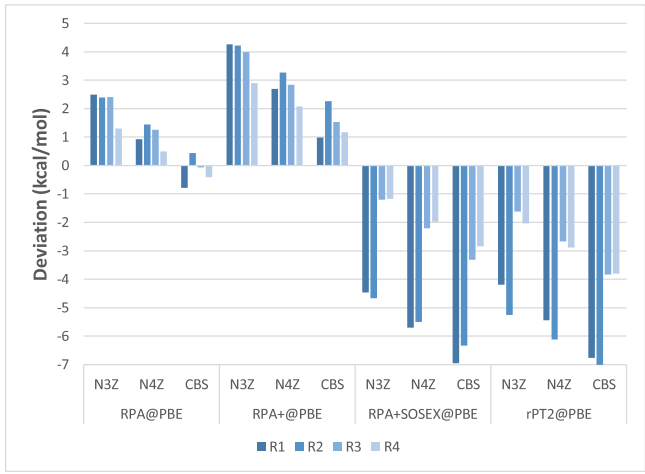

(a)

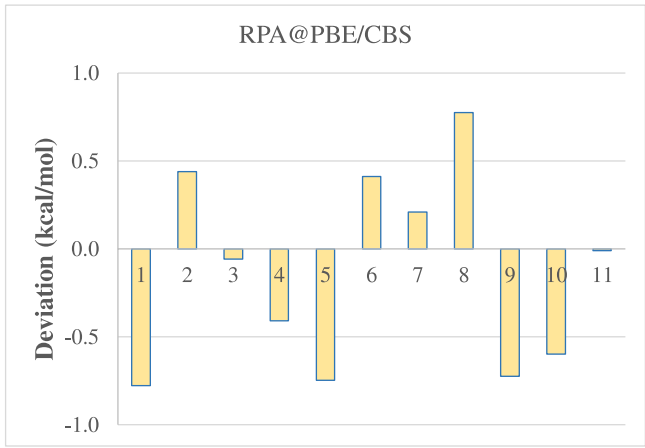

(b)

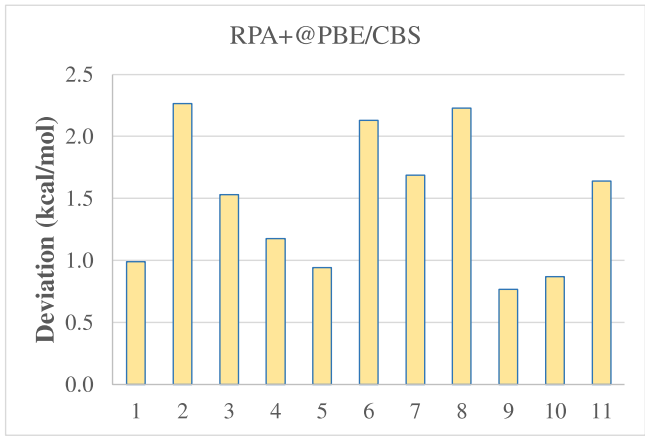

(c)

FIG. 4. (a) Deviations of calculated RPA, RPA+, RPA+SOSEX, and rPT2@PBE energies from reference energies[64] for 4 reactions (R1, R2, R3, and R4) in DARC test set. These errors are extrapolated to the complete basis set (CBS) from results calculated with NAO-VCC-3*Z* (abbreviated as N3Z) and NAO-VCC-4*Z* (abbreviated as N4Z) basis sets. Since the rSE corrections are very similar to RPA, the error bars of rSE are not shown here. (b) Deviations of calculated RPA@PBE/CBS energies from reference energies[64] for 11 reactions in DARC test set. These errors are extrapolated to the complete basis set (CBS) from results calculated with NAO-VCC-3*Z* (abbreviated as N3Z) and NAO-VCC-4*Z* (abbreviated as N4Z) basis sets. (c) Deviations of calculated RPA+@PBE/CBS energies from reference energies[64] for 11 reactions in DARC test set. These errors are extrapolated to the complete basis set (CBS) from results calculated with NAO-VCC-3*Z* (abbreviated as N3Z) and NAO-VCC-4*Z* (abbreviated as N4Z) basis sets.

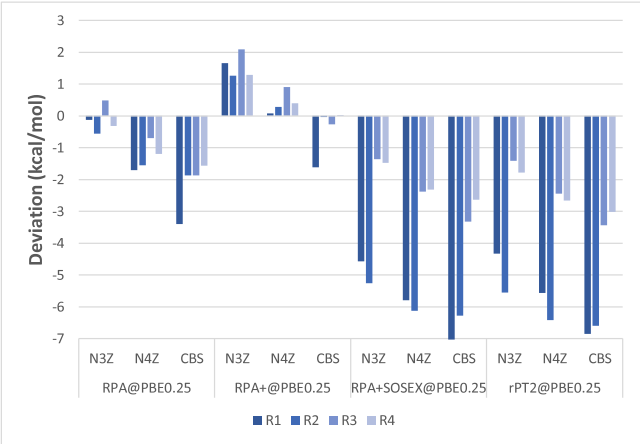

FIG. 5. Deviations of calculated RPA, RPA+, RPA+SOSEX, and rPT2@PBE0.25 energies from reference energies[64] for 4 reactions (R1, R2, R3, and R4) in DARC test set. These errors are extrapolated to the complete basis set (CBS) from results calculated with NAO-VCC-3Z (abbreviated as N3Z) and NAO-VCC-4Z (abbreviated as N4Z) basis sets.

delocalization error should reflect in the reference orbitals. The difference between semilocal DFA and other methods with EXX was earlier attributed to the different description of the electron density hole or charges in HF and DFT.[65] The HF method is known to localize charges and therefore yields more compact electron density compared to PBE or exact electron density. Semilocal DFA (PBE-GGA) prefers delocalization of the charges, overstabilizing π-conjugated bonds of the reactants.

Our results show (Figure 6) that the error in HF method used as a reference in RPA leads to a relative destabilization of the reagents compared to the products causing systematic overbinding for RPA@HF. Comparison of RPA@PBE, RPA@PBE0, and RPA@HF results shows an increased sensitivity of the reaction binding energies causing a worsening in the results using an admixture of HF in the reference. It should be noted here that overbinding refers to the overstabilization of the products compared to the reagents. Overbinding then leads to more exothermic reaction.

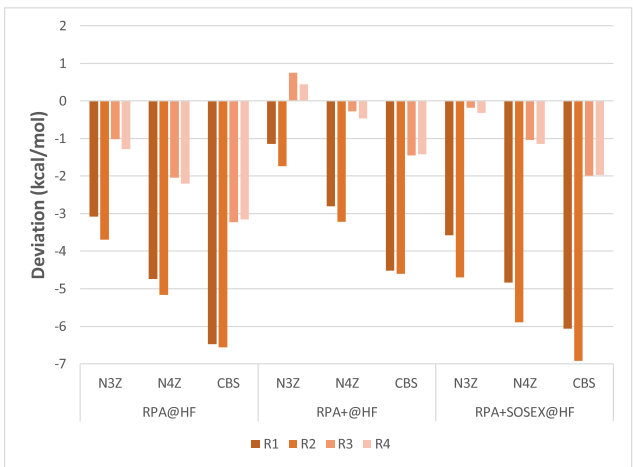

FIG. 6. Deviations of calculated RPA, RPA+, and RPA+SOSEX energies from reference energies[64] for 4 reactions (R1, R2, R3, and R4) in DARC test set. These errors are extrapolated to the complete basis set (CBS) from results calculated with NAO-VCC-3Z (abbreviated as N3Z) and NAO-VCC-4Z (abbreviated as N4Z) basis sets. Since the HF reference makes a zero SE contribution for SOSEX and rPT2 as well, we display RPA+SOSEX@HF only and not rPT2@HF.

Figure 4(a) shows that for RPA@PBE, the N3Z and N4Z basis set errors shift the reaction energies in the endothermic direction. N3Z and N4Z are short for NAO-VCC-3Z and NAO-VCC-4Z as shown on Figures 4(a)–6. After CBS extrapolation, the RPA@PBE energies show a good agreement with the reference energies. The reference energies are high-level CCSD(T)/CBS data.[64] RPA+@PBE at CBS limit has 1-3 kcal/mol endothermic error while the SOSEX@PBE and rPT2@PBE reaction energies are shifted in the exothermic direction up to 7 kcal/mol.

Figures 4(b) and 4(c) display the results for the full DARC test set (all 11 reactions) with RPA and RPA+@PBE. These plots confirm the applicability of RPA@PBE for the weak interactions in the DARC test set.

Figure 5 shows the deviations for PBE hybrid reference orbitals (PBE0.25) in a similar way as in Fig. 4(a). The basis set error again shifts the results in the endothermic direction while the more compact PBE0.25 reference orbitals shift the RPA and RPA+ reaction energies in the exothermic direction. The SOSEX and rPT2 energies are only slightly influenced by the changed reference orbitals. The best results are delivered by RPA+@PBE0.25 CBS as shown in Fig. 5.

Figure 6 shows that the errors for reactions 1 and 2 are very sensitive on the choice of the reference orbitals and the HF reference causes a large exothermic shift. Notice that for HF reference orbitals, SOSEX and rPT2 are equivalent.

The superiority of RPA@PBE results suggest that the reactions within the DARC test set are mostly dominated by the dispersion interaction. The role of SOSEX could be relevant if the delocalization/localization error dominates the reaction.

At last, we assess all many-body approximations from the aspect of self-interaction or delocalization error. The SIE11 data set can be now used to distinguish the performance of all our methods from their performance on weak interaction for the DARC test set. If the RPA improves the description of delocalization error, it should give similar performance for the SIE11 test set as it did for the DARC data set.

Semilocal density functionals are known to produce delocalization errors for dissociation and localization error for static or strong correlation. The RPA@PBE displays a self-correlation error, but it gives the correct spin-symmetry-unbroken dissociation for the H_2 molecule, a prototype of static correlation.

Our results confirm (Table VII) that RPA gives overall better accuracy for the reaction energies than semilocal functionals.[85] The reference energies were computed at the level of CCSD(T)/CBS.[64,86] It should be noted here that very large errors were obtained for the dissociation of FLiF with all approximations assessed in Ref. 85. The performance of RPA@PBE is overall comparable to hybrid functionals.

Compared to the DARC data set, the accuracy of the RPA@PBE is worse for the SIE11 tests set. The CBS extrapolated deviations of the SIE11 reaction energies are displayed in Table VII.

TABLE VII. The deviations of CBS extrapolated SIE11 reaction energies from reference CCSD(T)/CBS energies.[64] Errors are given in kcal/mol.

Reagents	Products	Reference	RPA	RPA+	SOSEX	RPA+rSE	rPT2
He_2^+	$He + He^+$	57.44	13.31	13.49	−6.13	14.20	−3.95
$(NH_3)_2^+$	$NH_3 + NH_3^+$	35.34	4.65	4.25	−6.21	6.56	−3.45
$(H_2O)_2^+$	$H_2O + H_2O^+$	37.25	9.91	9.53	−8.97	12.34	−5.63
$(C_4H_{10})^+$	$C_2H_5 + C_2H_5^+$	35.28	2.25	1.52	−5.14	5.45	−2.50
$(CH_3)_2^+$	$CH_3 + CH_3CO^+$	22.57	1.34	0.53	0.02	4.06	4.52
ClFCl	ClClF	−1.01	5.64	5.24	−10.15	5.18	−6.41
$C_2H_4\cdots F_2$	$C_2H_4 + F_2$	1.08	−3.02	−3.11	−3.39	−0.08	−0.08
$C_6H_6\cdots Li$	$C_6H_6 + Li$	9.5	−8.19	−9.59	−7.34	−9.11	−5.57
$NH_3\cdots ClF$	$NH_3 + ClF$	10.5	−0.88	−1.29	−2.53	0.32	1.97
NaOMg	MgO + Na	69.56	−5.55	−6.66	8.51	−10.47	7.73
FLiF	$Li + F_2$	94.36	47.49	46.20	−24.99	46.25	−23.33
		MD	6.08	5.47	−6.03	6.79	−3.34
		MAD	9.29	9.22	7.58	10.36	5.92
		CSSD	15.14	15.08	8.09	15.15	8.02
		Min	−8.19	−9.59	−24.99	−10.47	−23.33
		Max	47.49	46.20	8.51	46.25	7.73

The difference in accuracy arises from the different performance of the RPA for the van der Waals interactions and delocalization error. RPA has 100% exact exchange but is infected by self-correlation. This could be improved by SOSEX; however, SOSEX gives about the same error as RPA but with an opposite sign. SOSEX is not designed to capture weak interactions as clearly shows up for the DARC test set. However, SOSEX generally cannot be used either to account for delocalization error. The rPT2@PBE gives significantly better accuracy for the SIE11 test set than SOSEX does. Surprisingly, the RPA+@PBE provides reasonable results almost in the error range of hybrid functionals. RPA+ rSE is similar to RPA in performance. Apparently, the rPT2 gives the best performance, reaching the accuracy of the best hybrid functional M08-HF.

CONCLUSIONS

Three different sets of reaction groups were assessed and compared from different aspects. Each set of reactions represents different challenges for electronic structure approximations. At first, we compare the consistency of several many-body approximations, testing reaction energies of the RC*n* reaction classes. An accurate method should display consistently improved results for higher levels of the hierarchy. RPA gives very large errors for atomization reactions. A significant improvement with RPA@PBE is noticed for the isogyric test set. For atomization reactions, the large error in RPA can be improved by the inclusion of the SOSEX correction. According to our results for isogyric reactions, the RPA+SOSEX shows inconsistency; therefore, the SOSEX itself is not recommended as a universal approximation. The rPT2 method which in contrast to the SOSEX method includes single excitations too, is more consistent.

The DARC test set is a part of the larger GMTKN30 data set. The poor results of semilocal density functionals for the reactions in the DARC test set were attributed to three effects: delocalization or localization error and the lack of dispersion correction. In this work, we clarify the picture. The accurate RPA@PBE results are evidence of the dominant role of weak intramolecular interactions in these reactions. Neither SOSEX nor rPT2 gives any improvement beyond RPA.

In all our tests, we prefer to apply RPA@PBE. The choice is very well justified especially for the DARC reactions test. RPA@PBE provides far the best accuracy for this data set. The conclusion from the results is relevant. The inclusion of the HF in the reference of RPA deteriorates the results, confirming that dispersion interactions govern the reactions of the DARC set.

Finally, the SIE11 test set confirms that the self-interaction or delocalization error clearly needs the "beyond-RPA" treatment, as confirmed by the best performance of the rPT2 approximation. Our result show that overall the rPT2 approximation gives good accuracy in most tests. In certain tests, the rPT2 method's wider applicability can be somewhat limited by the SOSEX approach. The results also provide some hint for the need of an intrinsic kernel correction to the RPA.

ACKNOWLEDGMENTS

This work was supported by the Department of Energy under Grant No. DE- SC0010499. A.R. appreciates helpful discussions with G. I. Csonka and P. D. Mezei.

[1]W. Kohn and L. J. Sham, Phys. Rev. **140**, A1133 (1965).
[2]R. G. Parr and W. Yang, *Density-Functional Theory of Atoms and Molecules* (Oxford University Press, Oxford, 1989); W. Koch and M. C. Holthausen, *A. Chemist*s Guide to Density Functional Theory* (Wiley-VCH, New York, 2001).
[3]A. D. Becke, J. Chem. Phys. **98**, 5648 (1993).
[4]K. Raghavachari, B. B. Stefanov, and L. A. Curtiss, Mol. Phys. **91**, 555 (1997).
[5]L. A. Curtiss, K. Raghavachari, P. C. Redfern, and J. A. Pople, J. Chem. Phys. **112**, 7374 (2000).
[6]B. J. Lynch, P. L. Fast, M. Harris, and D. G. Truhlar, J. Phys. Chem. A **104**, 4811 (2000).
[7]Y. Zhao, O. Tishchenko, and D. G. Truhlar, J. Phys. Chem. B **109**, 19046 (2005).
[8]Y. Feng, L. Liu, J.-T. Wang, H. Huang, and Q.-X. Guo, J. Chem. Inf. Comput. Sci. **43**, 2005 (2003).

[9]P. C. Redfern, P. Zapol, L. A. Curtiss, and K. Raghavachari, J. Phys. Chem. A **104**, 5850 (2000).
[10]S. Grimme, Angew. Chem., Int. Ed. **45**, 4460 (2006).
[11]S. Grimme, Org. Lett. **12**, 4670 (2010).
[12]P. R. Schreiner, A. A. Fokin, R. A. Pascal, Jr., and A. de Meijere, Org. Lett. **8**, 3635 (2006).
[13]R. Huenerbein, B. Schirmer, J. Moellmann, and S. Grimme, Phys. Chem. Chem. Phys. **12**, 6940 (2010).
[14]A. Ruzsinszky, J. P. Perdew, G. I. Csonka, O. A. Vydrov, and G. E. Scuseria, J. Chem. Phys. **126**, 104102 (2007).
[15]A. Ruzsinszky, J. P. Perdew, G. I. Csonka, O. A. Vydrov, and G. E. Scuseria, J. Chem. Phys. **125**, 194112 (2006).
[16]S. Grimme, J. Comput. Chem. **25**, 1463 (2004).
[17]S. Grimme, J. Comput. Chem. **27**, 1787 (2006).
[18]S. Grimme, J. Antony, S. Ehrlich, and H. Krieg, J. Chem. Phys. **132**, 154104 (2010).
[19]J. F. Dobson, J. Wang, B. P. Dinte, K. McLennan, and H. M. Le, Int. J. Quantum Chem. **101**, 579 (2005).
[20]A. J. Cohen, P. Mori-Sanchez, and W. Yang, Chem. Rev. **112**, 289 (2012).
[21]A. J. Cohen, P. Mori-Sanchez, and W. Yang, Science **321**, 792 (2008).
[22]J. P. Perdew and A. Zunger, Phys. Rev. B **23**, 5048 (1981).
[23]P. Mori-Sanchez, A. J. Cohen, and W. Yang, Phys. Rev. Lett. **100**, 146401 (2008).
[24]P. Mori-Sanchez, A. J. Cohen, and W. Yang, Phys. Rev. A **85**, 042507 (2012).
[25]M. D. Wodrich, C. S. Wannere, Y. Mo, P. D. Jarowski, K. N. Houk, and P. v. R. Schleyer, Chem.–Eur. J. **12**, 7731 (2007).
[26]M. D. Wodrich, C. Corminboeuf, and P. von Rague Schleyer, Org. Lett. **8**, 3631 (2006).
[27]P. R. Schreiner, Angew. Chem., Int. Ed. **46**, 4217 (2007).
[28]H. Eshuis, J. E. Bates, and F. Furche, Theor. Chem. Acc. **131**, 1084 (2012).
[29]F. Furche, Phys. Rev. B **64**, 195120 (2001).
[30]D. C. Langreth and J. P. Perdew, Phys. Rev. B **21**, 5469 (1980).
[31]F. Furche and T. Van Voorhis, J. Chem. Phys. **122**, 164106 (2005).
[32]J. P. Perdew, V. N. Staroverov, J. Tao, and G. E. Scuseria, Phys. Rev. A **78**, 052513 (2008), and references therein.
[33]A. Ruzsinszky, J. P. Perdew, and G. I. Csonka, J. Chem. Theory Comput. **6**, 127 (2010).
[34]J. Harl and G. Kresse, Phys. Rev. B **77**, 045136 (2008).
[35]Z. Yan, J. P. Perdew, and S. Kurth, Phys. Rev. B **61**, 16430 (2000).
[36]X. Ren, P. Rinke, C. Joas, and M. Scheffler, J. Mater. Sci. **47**, 7447 (2012).
[37]T. M. Henderson and G. E. Scuseria, Mol. Phys. **108**, 2511 (2010).
[38]G. E. Scuseria, T. M. Henderson, and D. C. Sørensen, J. Chem. Phys. **129**, 231101 (2008).
[39]A. Grüneis *et al.*, J. Chem. Phys. **131**, 154115 (2009).
[40]J. Paier, B. G. Janesko, T. M. Henderson, G. E. Scuseria, A. Grüneis, and G. Kresse, J. Chem. Phys. **132**, 094103 (2010); **133**, 179902 (2010).
[41]X. Ren, A. Tkatchenko, P. Rinke, and M. Scheffler, Phys. Rev. Lett. **106**, 153003 (2011).
[42]A. Heßelmann, Phys. Rev. A **85**, 012517 (2012).
[43]A. Heßelmann, Top. Curr. Chem. **365**, 97 (2015).
[44]B. Mussard, P. Reinhardt, J. G. Ángyán, and J. Toulouse, J. Chem. Phys. **142**, 154123 (2015).
[45]J. Bates and F. Furche, J. Chem. Phys. **139**, 171103 (2013).
[46]L. A. Curtiss, K. Raghavachari, P. C. Redfern, and J. A. Pople, J. Chem. Phys. **106**, 1063 (1997).
[47]B. J. Lynch and D. G. Truhlar, J. Phys. Chem. A **107**, 8996 (2003).
[48]A. Tajti, P. G. Szalay, A. G. Császár, M. Kállay, J. Gauss, E. F. Valeev, B. A. Flowers, J. Vázquez, and J. F. Stanton, J. Chem. Phys. **121**, 11599 (2004).
[49]Y. Zhao, B. J. Lynch, and D. G. Truhlar, J. Phys. Chem. A **108**, 2715 (2004).
[50]Y. Zhao, N. González-García, and D. G. Truhlar, J. Phys. Chem. A **109**, 2012 (2005).
[51]Y. Zhao and D. G. Truhlar, J. Chem. Phys. **125**, 194101 (2006).
[52]M. Hellgren, D. R. Rohr, and E. K. U. Gross, J. Chem. Phys. **136**, 034106 (2012).
[53]M. Hellgren, F. Caruso, D. R. Rohr, X. Ren, A. Rubio, M. Scheffler, and P. Rinke, Phys. Rev. B **91**, 165110 (2015).
[54]R. J. Bartlett, I. Grabowski, S. Hirata, and S. Ivanov, J. Chem. Phys. **122**, 034104 (2005).
[55]D. Feller, K. A. Peterson, and T. D. Crawford, J. Chem. Phys. **124**, 054107 (2006).
[56]S. E. Wheeler, K. N. Houk, P. v. R. Schleyer, and W. D. Allen, J. Am. Chem. Soc. **131**, 2547 (2009).
[57]W. J. Hehre, L. Radom, P. v. R. Schleyer, and J. A. Pople, *Ab Initio Molecular Orbital Theory* (Wiley-Interscience, New York, 1986).
[58]W. J. Hehre, R. Ditchfield, L. Radom, and J. A. Pople, J. Am. Chem. Soc. **92**, 4796 (1970).
[59]L. Radom, W. J. Hehre, and J. A. Pople, J. Am. Chem. Soc. **93**, 289 (1971).
[60]D. W. Rogers, A. Podosenin, and J. F. Liebman, J. Org. Chem. **58**, 2589 (1993).
[61]P. v. R. Schleyer, P. K. Freeman, H. Jiao, and B. Goldfuss, Angew. Chem., Int. Ed. **34**, 337 (1995).
[62]P. George, M. Trachtman, C. W. Bock, and A. M. Brett, Theor. Chem. Acc. **38**, 121 (1975).
[63]B. A. Hess, Jr. and L. J. Schaad, J. Am. Chem. Soc. **93**, 305 (1971).
[64]L. Goerigk and S. Grimme, J. Chem. Theory Comput. **7**, 291 (2011).
[65]E. R. Johnson, P. Mori-Sanchez, A. J. Cohen, and W. Yang, J. Chem. Phys. **129**, 204112 (2008).
[66]J. Noga, W. Kutzelnigg, and W. Klopper, Chem. Phys. Lett. **199**, 497 (1992).
[67]D. P. Tew, W. Klopper, and T. J. Helgaker, Comput. Chem. **28**, 1307 (2007).
[68]D. E. Woon and T. H. Dunning, J. Chem. Phys. **103**, 4572 (1995).
[69]K. A. Peterson and T. H. Dunning, J. Chem. Phys. **117**, 10548 (2002).
[70]I. Y. Zhang, X. G. Ren, P. Rinke, V. Blum, and M. Scheffler, New J. Phys. **15**, 123033 (2013).
[71]A. K. Wilson, T. van Mourik, and T. H. Dunning, J. Mol. Struct.: THEOCHEM **388**, 339 (1996).
[72]K. L. Schuchardt, B. T. Didier, T. Elsethagen, L. Sun, V. Gurumoorthi, J. Chase, J. Li, and T. L. Windus, J. Chem. Inf. Model. **47**, 1045 (2007).
[73]V. Blum, F. Hanke, R. Gehrke, P. Havu, V. Havu, X. Ren, K. Reuter, and M. Scheffler, Comput. Phys. Commun. **180**, 2175 (2009).
[74]X. Ren, P. Rinke, V. Blum, J. Wieferink, A. Tkatchenko, A. Sanfilippo, K. Reuter, and M. Scheffler, New J. Phys. **14**, 053020 (2012).
[75]H. Eshuis, J. Yarkony, and F. Furche, J. Chem. Phys. **132**, 234114 (2010).
[76]J. Harl, L. Schimka, and G. Kresse, Phys. Rev. B **81**, 115126 (2010).
[77]H. Eshuis and F. Furche, J. Chem. Phys. **136**, 084105 (2012).
[78]G. I. Csonka and J. Kaminsky, J. Chem. Theory Comput. **7**, 988 (2011).
[79]T. Helgaker, W. Klopper, H. Koch, and J. Noga, J. Chem. Phys. **106**, 9639 (1997).
[80]A. Halkier, T. Helgaker, P. Jorgensen, W. Klopper, H. Koch, J. Olsen, and A. K. Wilson, Chem. Phys. Lett. **286**, 243 (1998).
[81]F. Della Sala, Theor. Chem. Acc. **131**, 278 (2012).
[82]P. Mezei, G. I. Csonka, and A. Ruzsinszky, J. Chem. Theory Comput. **11**, 3961 (2015).
[83]F. Jensen, Theor. Chem. Acc. **113**, 187 (2005).
[84]H. Eshuis and F. Furche, J. Phys. Chem. Lett. **2**, 983 (2011).
[85]Y. Zhao and D. G. Truhlar, J. Chem. Theory Comput. **7**, 669 (2011).
[86]P. Jurečka and P. Hobza, Chem. Phys. Lett. **365**, 89 (2002).